



# Characterisation of pre-industrial hybrid cement and effect of pre-curing temperature



Bo Qu <sup>a, b, \*</sup>, A. Martín <sup>a</sup>, J.Y. Pastor <sup>a</sup>, A. Palomo <sup>b</sup>, A. Fernández-Jiménez <sup>b</sup>

<sup>a</sup> Department of Materials Science, CIME Technical University of Madrid, E28040, Madrid, Spain

<sup>b</sup> Eduardo Torroja Institute for Construction Science (C.S.I.C.), E28033, Madrid, Spain

## ARTICLE INFO

### Article history:

Received 22 March 2016

Accepted 27 July 2016

Available online 30 July 2016

### Keywords:

Hybrid cements

Curing temperature

NMR

## ABSTRACT

This study aimed to determine the physical-mechanical, mineralogical and microstructural properties of a pre-industrially manufactured hybrid cement (HYC) containing 5% alkaline activator and less than 30% clinker. The effect of the initial curing temperature ( $25 \pm 1$  or  $85 \text{ }^\circ\text{C}$  for 20 h) on hydration kinetics and the development of compressive strength were also explored. The hydration products formed were characterised using XRD, SEM/EDX and  $^{27}\text{Al}$  and  $^{29}\text{Si}$  MAS-NMR. The findings showed that pre-industrial hybrid cement sets when hydrated with water and hardens to a 28-day mechanical strength of 35 MPa. The main reaction product formed was a mix of cementitious gels: C-(A)-S-H and C-A-S-H. Curing at  $85 \text{ }^\circ\text{C}$  for 20 h, shows a behaviour similar to OPC, inhibited ettringite formation and generated more polymerised gels, enhancing 3-day but not 28- or 90-day mechanical strength.

© 2016 Elsevier Ltd. All rights reserved.

## 1. Introduction

Since Portland cement (OPC) was patented in the nineteenth century, its use has spread worldwide, making it one of humanity's most prevalent structural materials. That predominance is attributable to its low cost, high mechanical strength and universal availability [1,2]. Today, however, the cement industry is faced with higher production costs due to: i) rising energy prices worldwide, which are mirrored nearly linearly in cement costs; ii) shortage of supply of quality raw materials; and iii) the need to reduce CO<sub>2</sub> emissions (OPC manufacture generates nearly two billion tonnes/year of CO<sub>2</sub> emissions, accounting for 8–10% of anthropogenic emissions worldwide [3]). As a result, both the scientific and technical communities are working to develop alternative cements and binders [1,4–6].

One effective way of lowering the CO<sub>2</sub> emissions associated with OPC manufacture is to use the so-called alkaline cements or geopolymers [4–7] developed in recent decades. Any contention that alkaline cements can replace OPC in all of its many applications at this time is hardly realistic, however. One possible intermediate solution (with scant technical, logistic or economic implications)

might consist in reducing the clinker content in cement as far as possible and expanding the use of supplementary cementitious materials (SCMs) such as natural pozzolans or industrial by-products (fly ash or slag) [8–11]. The problem posed by using large amounts of SCMs, however, is that they lengthen setting times and lower the initial mechanical strength of mortars and concretes. As in alkaline cement production, solid or liquid activators (new admixtures developed for this purpose) can be used to circumvent that problem. The combination of traditional OPC and alkaline cements yields what are known as hybrid cements (HYC) [5,12,13].

Hybrid cements are the result of alkali-activating low (20–30%) clinker content blended cements with an alkaline activator added in a proportion of approximately 5%. The remaining 65–75% of the blend consists of supplementary cementitious materials (SCMs), either natural pozzolans or industrial by-products such as fly ash from coal-fired power plants or blast furnace slag. In Europe, the amount of supplementary materials (SCMs) that can be used as additions in Portland cement is limited by the existing legislation (EN 197-1). Elsewhere, however, such as in the USA (ASTM standard C1157/C1157M-11) and certain Latin American countries (as Colombia, NTC 121), neither the chemical composition of cements nor of their components are restricted. As the standards in place there classify cements on the grounds of prescriptive and performance requirements, hybrid cements meeting those requirements could be commercialised immediately in such countries.

Alkaline activators (admixtures) are used in hybrid cements to

\* Corresponding author. Department of Materials Science, CIME Technical University of Madrid, E28040, Madrid, Spain.

E-mail address: [qubo@mater.upm.es](mailto:qubo@mater.upm.es) (B. Qu).

hasten the initial SCM reactions. Moreover, solid alkaline activators such as deployed in this study feature an important additional technological advantage, for with them hybrid cement can be produced using traditional Portland cement manufacturing processes. Jointly milling clinker + SCMs + activator yields a powdery material that has merely to be mixed with water to set and harden [13,14]. The production of such cements (hereafter “hybrid cements”) therefore calls for an in-depth understanding of both traditional (OPC) and alkaline cement behaviour.

The type of reaction products formed in alkaline cement would be expected to depend largely on the reaction conditions: chemical composition of the starting materials, type and concentration of the alkaline activator and initial curing conditions, among others [4–7]. Two types of alkaline cements can be distinguished. **a)** In the alkaline activation of blast furnace slag (AABFS), temperature hastens initial strength development (as in OPC), although strength declines at more mature ages [15–17]. The C-A-S-H gel formed, as well as the secondary reaction products, are more crystalline than when heat is not applied. **b)** In the alkaline activation of fly ash (AAFA), curing temperature (between 65 and 90 °C) plays a very important role, as heat accelerates early age reactions, with the product exhibiting 1-day mechanical strength upward of 30 MPa [18,19].

Curing at a higher temperature, for instance, is known to expedite initial OPC hydration. The C-S-H gel formed during OPC hydration at temperatures >65 °C is more highly polymerised than when it forms at ambient temperature [20–22].

The effect of curing temperature on hybrid cements has not yet been studied, however. The present survey therefore pursued a dual objective. i) On the one hand, it aimed to verify the mechanical properties, composition and structure of the reaction products formed during the hydration of pre-industrially manufactured hybrid cement; ii) and on the other, to determine whether pre-curing temperature (25 ± 1 or 85 °C) plays a significant role in hydration.

## 2. Experimental procedure

### 2.1. Materials

The pre-industrial hybrid cement used was manufactured in at Latin-American cement plant (about 20 tons were manufacture).

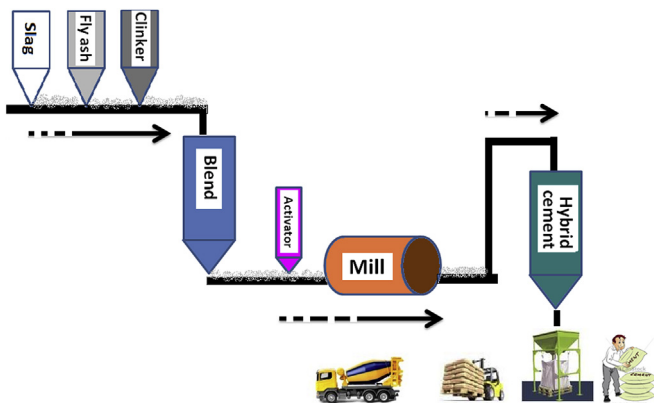


Fig. 1. Stages in HYC manufacture.

Table 1

Chemical composition of the pre-industrial hybrid cement (% by mass).

	CaO	SiO <sub>2</sub>	Al <sub>2</sub> O <sub>3</sub>	Fe <sub>2</sub> O <sub>3</sub>	MnO/Mn <sub>2</sub> O <sub>3</sub>	MgO	SO <sub>3</sub>	Na <sub>2</sub> O	K <sub>2</sub> O	TiO <sub>2</sub>	Other	<sup>b</sup> Lol
<sup>a</sup> CEMCC5	39.67	32.53	12.2	3.83	0.804	0.94	3.12	1.04	0.78	0.5	1.899	2.32

<sup>a</sup> CEM CC5 = pre-industrially manufactured hybrid cement.

<sup>b</sup> Lol, loss on ignition.

The process, consisting in the joint milling of Portland clinker, slag, fly ash and activator, is depicted in Fig. 1. The proportions used were 30% Portland cement clinker +32.5% BFS +32.5% FA +5% solid activator.

Table 1 gives the chemical composition of the pre-industrial hybrid cement (denominated CEM CC5) as determined on a Bruker S8 TIGER X-ray fluorescence analyser. Its mineralogy was found with a BRUKER AXS D8 ADVANCE X-ray diffractometer (XRD) and quantified using Rietveld refinement. Given the high vitreous content of pre-industrial hybrid cement, its quantification was based on an external standard (30% corundum) [23]. Particle size distribution was determined by laser granulometry using a SYMPATEC diffractometer with a measuring range of 0.90–175 μm. The powdery samples were dispersed with isopropyl alcohol to eliminate inter-particle Van der Waals and electrostatic forces.

The Rietveld-refined XRD pattern for the hybrid cement (CC5) is reproduced in Fig. 2 (30% corundum was used as a standard [23]). The quantification findings are given in Table 2. The clinker content in the pre-industrial hybrid cement appeared to be slightly higher than stipulated (on the order of 32.5% rather than the 30% specified).

Further to the particle size distribution findings shown in Fig. 3, 95% of the particles measured under 45 μm and 40% under 10 μm, meeting an important requirement for reactivity.

### 2.2. Method

In some Latin-American countries as Venezuela, Mexico, Colombia the standards are more similar to ASTM than the EN standards. For example in Colombia, the performance specification for hydraulic cement, standard NTC 121 (equivalent to ASTM C1157/C1157M.11), was approved in 2014. This standard classifies cement types by their features and performance. General purpose cement, UG, for instance, must exhibit a Vicat needle-determined initial

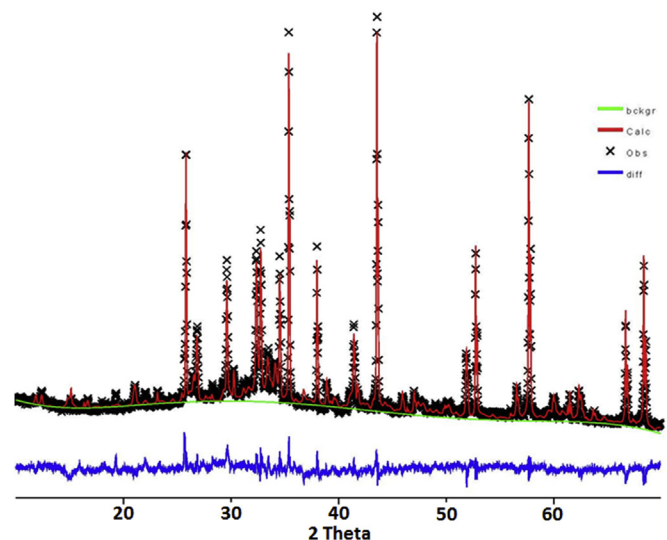


Fig. 2. Rietveld quantification of the cement CC5 studied using 30% corundum as a standard.

**Table 2**  
Rietveld quantification of cement mineralogy (using 30% corundum as a standard).

Rietveld (%)	Hybrid cement	
	%	Sub-total
C <sub>3</sub> S	20.05	32.50
C <sub>2</sub> S	5.45	
C <sub>3</sub> A	3.98	
C <sub>4</sub> AF	3.02	
Gypsum	1.70	
Quartz	3.00	63.75
Mullite	6.27	
Amorphous matter	54.48	

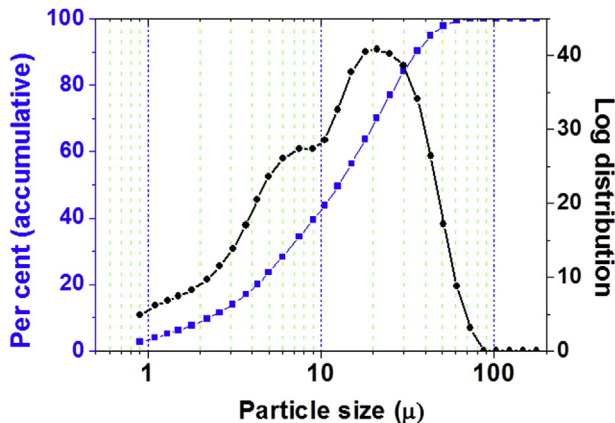


Fig. 3. Particle size distribution in cement.

setting time of over 45 and under 420 min. In the present study, however, setting time was found as specified in European standard EN 196-3, which is practically the same as in the Colombian code and in ASTM 191.

In some Latin-American country as Colombian standard NTC 220 stipulates the use of 5-cm cubic specimens (with a cement/sand ratio of 1/2.75, the amount of mixing water should be one that produces a flow of  $110 \pm 5$  in 25 strokes with the flow table) to determine mechanical strength. The minimum 3-, 7- and 28-day compressive strength values required for general purpose hydraulic cement (UG) are 8, 15 and 24 MPa, respectively (NTC 121). Similar specifications about the specimens manufacture and compressive strength values are in Venezuela standards (COVENIN 484-89 and COVENIN 28-93) or Mexico standards (NMX-C-061-ONNCE-2010 NMX-C-414-ONNCE-2014).

In the present study, however, prismatic ( $4 \times 4 \times 16$  cm) mortar specimens were prepared as per standard EN 196-1 (water/cement ratio = 0.5; sand/cement = 3/1), which is nearly equivalent to standards ASTM C348 and NTC 120.

Two pre-curing temperatures were used to determine the effect of temperature during initial curing of hybrid cement: a)  $25 \pm 1$  °C at 99% RH for 20 h (further to EN 196-1); b) 85 °C at 99% RH for 20 h (conditions normally used to alkali-activate fly ash [5,19]). After pre-curing, the material was removed from the moulds and stored in a curing chamber ( $25 \pm 1$  °C and 99% RH) until the test age (3, 28 or 90 days).

Hydration kinetics at 25 °C and 85 °C were determined by isothermal conduction calorimetry on a THERMOMETRIC TAM Air calorimeter. To that end, 5 g of cement were hydrated with water at a water/cement ratio of 0.5 (mass), mixed by hand for 3 min and then placed in the calorimeter.

The prismatic ( $1 \times 1 \times 6$ -cm) paste specimens prepared with a water/cement ratio of 0.3 to determine setting times were also used

for mineralogical and microstructural characterisation (XRD, FTIR SEM/EDX and <sup>29</sup>Si, <sup>27</sup>Al MAS NMR). At the specified age, the pastes were milled to a fine powder and the hydration reactions were detained with acetone and ethanol.

The X-ray diffraction patterns for the powdered samples were recorded on a Philips diffractometer using CuK $\alpha_{1,2}$  radiation. The settings were: variable 6-mm divergence slit; 2 theta, 5–60°; step time, 0.5 s; step size, 0.02°. Selected samples were analysed with SEM/EDX techniques, in which polished and carbon-coated thin sections were studied under a JEOL JSM scanning electron microscope fitted with a solid-state BSE detector and a LINK-ISIS energy dispersive X-ray (EDX) analyser. The MAS NMR analyses were conducted on a Bruker Avance-400 spectrometer under the following conditions: <sup>29</sup>Si resonance frequency, 79.5 MHz; spinning rate, 10 kHz; pulse sequence, single pulse (5  $\mu$ s); recycle delay, 10 s; number of transients, 4912; external standard, TMS (tetramethylsilane); <sup>27</sup>Al resonance frequency, 104.3 MHz; spinning rate, 10 kHz; recycle delay, 5 s; pulse sequence, single pulse (2  $\mu$ s); number of transients, 400; external standard, Al(H<sub>2</sub>O)<sub>6</sub><sup>3+</sup>.

### 3. Results and discussion

#### 3.1. Reaction kinetics

The heat flow (J/g h) and total heat released (J/g) during pre-industrial hybrid cement hydration are plotted in Fig. 4 for pre-curing temperatures of 25 and 85 °C. A comparison of the heat output rate profiles reveals that both temperatures have profiles similar to that of a normal PC and so similar terminology is used in their interpretation here. Pre-induction occurred too quickly for the respective peaks to be visible on these curves.

At 25 °C, the acceleration-deceleration curve observed after a short induction period, with a peak at 10.8 h, was associated with the precipitation of reaction products [14,24–26]. The rounded form of the curve suggested a series of overlapping reactions (clinker hydration and slag and fly ash activation). These reactions induced fairly low heat of reaction, around 200 J/h. A higher pre-curing temperature expedited the hydration rate of cement considerably: at 85 °C the main band peaked at 2.2 h with a heat flow of 225 J/g h and clearly greater heat intensity.

It is clear from Fig. 4, that, with increasing temperature, the maximum hydration peak increases, while the time to reach the peak decreases. Additionally, it is observed that the peak width decreases with increasing temperature, indicating a faster hydration rate with time. This means, that the rate of cement and the SCMs hydration is accelerated with temperature, consistent with

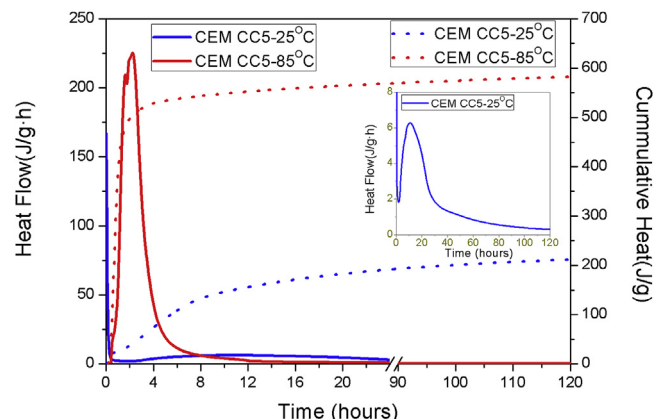


Fig. 4. Heat flow and total heat released by hybrid cement pre-cured at 25 or 85 °C.

the laws of chemical kinetics and may also explain the maximum total heat plateau occurring faster with temperature. It can also be observed in Fig. 4 that the accumulated total heat increases with temperature, it is probably due to more hydration products at early age are precipitated.

### 3.2. Setting time and mechanical strength

Table 3 gives the initial and final setting times for cement pre-cured at 25 °C. According to these findings, the hybrid cement (CEM CC5) exhibited setting times compliant with both European standard EN 196-1 (initial time > 75 min) and Colombian standard NTC 121 (between 45 and 420 min).

Fig. 5 shows the 3-, 28- and 90-day compressive strength for the (4 × 4 × 16-cm) prismatic mortar specimens pre-cured at 25 °C or 85 °C. Strength clearly rose with time. Initial pre-curing at the higher temperature improved 3-day strength substantially. That effect declined in more mature specimens, however. The 28-day strength of the cement pre-cured at 25 °C was 35 MPa, while the 90-day value was 40 MPa. In contrast, while the specimens pre-cured at 85 °C exhibited 3-day compressive strength of 30 MPa, thereafter the value remained virtually flat, with only a slight rise.

With the strength values recorded (despite the use of 4 × 4 × 16-cm instead of 5-cm cubic specimens), the hybrid cement developed compressive strength high enough to be regarded as apt for general construction in some country as cement type UG in Colombia, further to national standard NTC 121. From the standpoint of its mechanical strength, it could also be classified as a Type 32.5 cement under European legislation. Nonetheless, given its low clinker content, according to standard EN 196-1, it would have to be classed as a Type V cement.

### 3.3. Mineralogical and microstructural characterisation

The diffractograms for the anhydrous cement and its 3-, 28- and 90-day hydrated pastes, pre-cured at 25 or 85 °C, are reproduced in

**Table 3**  
Setting time.

Name	L/S	Setting time	
		Initial	Final
CEM C	0.3	202 min	327 min

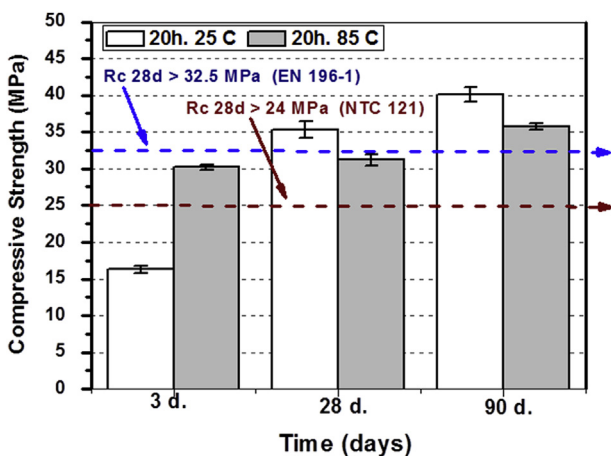


**Fig. 5.** Compressive strength of pre-industrial hybrid cement by reaction time and pre-curing temperature.

Fig. 6. In addition to the crystalline phases typical of clinker (such as alite and belite), the pattern for the starting cement exhibited the mullite and quartz present in the fly ash and a hump across 2θ 25–35°, associated with the vitreous component in the slag and ash.

An analysis of the variations in the diffractograms over time and by pre-curing temperature revealed the following.

- In the 25 °C specimens, the intensity of the diffraction lines associated with clinker anhydrous phases declined over time. In contrast, the lines associated with the quartz and mullite present in the fly ash remained unaltered. The new crystalline phases detected included portlandite, ettringite, calcite and a very low intensity signal associated with carboaluminates. Rather than rising over time, the intensity of the portlandite signal declined between 28 and 90 days. This was an indication that the fly ash not initially activated exhibited pozzolanicity at more mature ages [8,9].
- Portlandite, calcite and carboaluminates also appeared as new phases on the diffractograms for the cements pre-cured at 85 °C in the first 20 h. The most prominent difference between these diffractograms and the patterns for the cement pre-cured at 25 °C was the absence of ettringite, even after 90 days.
- All the diffractograms contained a hump from 25 to 35° which, as discussed below, was associated with the possible formation and precipitation of a mix of C-(A)-S-H/C-A-S-H gels. The precipitations of a mixture of gels has been demonstrated in previous works in blended cement [12–14] and compatibility studies of synthetic gels [27].

The <sup>27</sup>Al and <sup>29</sup>Si NMR-MAS spectra for the anhydrous cement and the 28-day pastes pre-cured at the two temperatures are reproduced in Fig. 7(a) and (b). The aluminium spectrum for the anhydrous cement contained a wide asymmetrical signal centred on +60 ppm with a shoulder at +80 ppm. The former was attributed to overlapping signals for the Al<sub>I</sub> present in the slag and fly ash [12,18,28] and the latter to the Al<sub>I</sub> in the clinker [29–31].

When the cement was hydrated, the intensity of the +80 ppm signal declined, the resonance at +60 ppm shifted to +58 ppm and

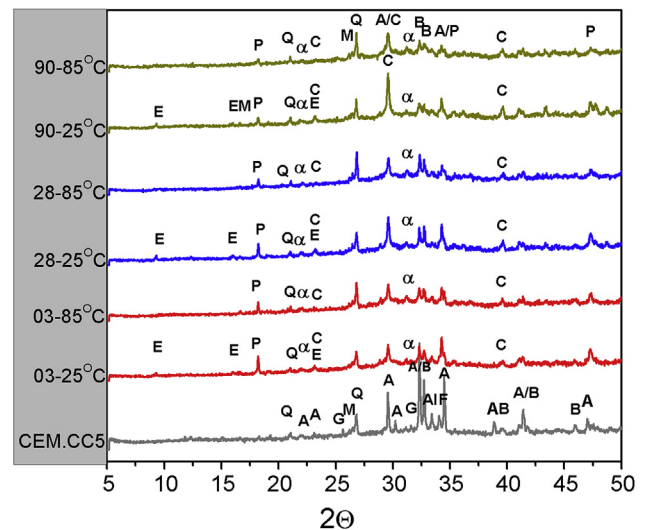


**Fig. 6.** Three-, 28- and 90-day XRD patterns for hybrid cement pre-cured at different temperatures. (Legend: A: alite 031-0301; Al: C<sub>3</sub>A 032-1048; B: belite 049-1673; C: calcite 081-2027; E: ettringite 041-1451; F: ferrite phase 030-0226; P: portlandite 044-1481; Q: quartz 046-1045; M: mullite 084-1205; G: CaSO<sub>4</sub>·2H<sub>2</sub>O 037-1496; α: 3CaO·Al<sub>2</sub>O<sub>3</sub>·0.5Ca(OH)<sub>2</sub>·0.5CaCO<sub>3</sub>·11.5H<sub>2</sub>O 041-0221).

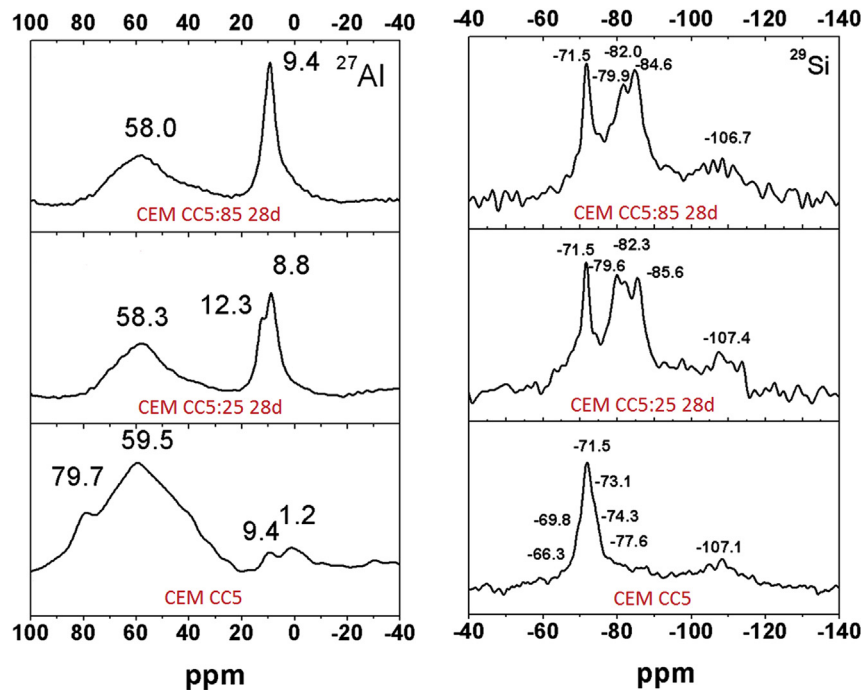


Fig. 7.  $^{27}\text{Al}$  MAS-NMR and  $^{29}\text{Si}$  MAS-NMR spectra for the anhydrous hybrid cement and its 28-day pastes.

new, very intense signals associated with octahedral aluminium ( $\text{Al}_\text{O}$ ) appeared at around 12–11 and 9–8 ppm. The signal at +58 ppm was attributed to the presence of tetrahedral Al ( $\text{Al}_\text{T}$ ), possibly surrounded by three or four silicon atoms [12,18,28]. The symmetry of this signal and the fact that it was narrower than the resonances in the starting materials suggested its possible association with the tetrahedral aluminium present in C-A-S-H- and (N,C)-A-S-H-like cementitious gels, as described in the literature [12–14,27].

The signal at around +12 ppm was attributed to the  $\text{Al}_\text{O}$  in the ettringite, likewise detected with XRD. The signals at around +8/+7 ppm may be associated with the presence of a small amount of octahedral Al ( $\text{Al}_\text{O}$ ) in the form of calcium carboaluminate [29–31]. This phase was also detected by XRD, where the low intensity of the signal was more than likely attributable to its scant crystallinity. The signal at +12.3 ppm was absent on the 85 °C spectrum and the signal at +8.8 shifted to +9.4 ppm. That finding confirmed that when the cement was pre-cured at 85 °C for 20 h, no ettringite formed (see spectrum deconvolution in Fig. 8).

The  $^{29}\text{Si}$  MAS-NMR spectrum (see Fig. 7(b)) for the anhydrous cement exhibited a narrow, symmetrical signal centred over –71.5 ppm and two shoulders, one at –70.2 and the other at –73.8 ppm, denoting monomers ( $\text{Q}^0$ ). The narrowest signal (–71.5 ppm) was attributed to belite ( $\text{C}_2\text{S}_{\text{ss}}$ ) and the other two to alite ( $\text{C}_3\text{S}_{\text{ss}}$ ) components. Alite and belite are the two main constituents of Portland clinker [29,30]. After spectrum deconvolution, a series of wide signals detected in addition to the aforementioned bands were assigned to the vitreous phase of the slag (see signals around –66, –74 and –77 ppm in Fig. 7 and Table 4) [28,31]. The lowest intensity signal centred at around –107/–108 ppm, along with the one at –89 ppm, were associated with components in the fly ash.

The signals associated with the anhydrous phases declined significantly on the 28-day silicon spectra and new signals appeared in the –79 to –90-ppm range. The signals at around –79, –82 and –85 ppm were respectively generated by  $\text{Q}^1$  (end-of-chain),  $\text{Q}^2$  (1Al) and  $\text{Q}^2$ (0Al) units, typical of C-(A)-S-H gels

[27,29,30]. The signals positioned at more negative values, around –87.9, –92 and –97.8 ppm (see Fig. 8 and Table 4), might be associated with  $\text{Q}^3$ (2Al),  $\text{Q}^3$ (1Al) and  $\text{Q}^3$ (0Al) units. The inference is that very complex, highly polymerised structures, possibly a mix of C-(A)-S-H and C-A-S-H gels, were forming in the per-industrial hybrid cement.

Pre-curing at 85 °C induce minor variations in the intensity of the signals comprising the 28-day gels. The ratio of less to more polymerised units ( $\text{Q}^1 + \text{Q}^2(\text{nAl})/\text{Q}^3(\text{nAl})$ ) was slightly higher in the material pre-cured at ambient temperature (2.9 compared to 2.5 at 85 °C). Extrapolating to C-(A)-S-H/C-A-S-H gel formation, this finding denoted the generation of more C-(A)-S-H gel in the cement pre-cured at ambient temperature and more C-A-S-H in the material pre-cured at 85 °C.

The pre-industrial hybrid cement exhibited a fairly low ( $\approx 40\%$ ) CaO content and a higher ( $\approx 12\%$ )  $\text{Al}_2\text{O}_3$  content than in OPC. Such circumstances would favour the uptake of Al in the linear silicon chains, which would in turn foster inter-chain cross-linking, giving rise to two-dimensional structures [12,28,29]. That result is consistent with the presence of a higher  $\text{Al}_\text{T}/\text{Al}_\text{O}$  ratio in these cements (see Fig. 9) than in ordinary portland cements. The signal at +58 ppm was an indication that in this case the  $\text{Al}_\text{T}$  was surrounded by several silicon atoms.

The 28-day samples studied under NMR were analysed with scanning electron microscopic (SEM/EDX) techniques to confirm the formation of one or several gels in the hybrid cement. The results are shown in Fig. 10. These micrographs showed that the materials pre-cured at both 25 and 85 °C had a fairly compact microstructure.

A number of unreacted spherical ash particles embedded in the 28-day cementitious matrix were observed. The clinker and slag particles were more difficult to distinguish morphologically. As the microanalyses show (Fig. 10, points 1, 2, 3 and 4), in addition to Ca and Si, the gel formed contained Al and some Na. The variations in gel composition were attributed to the fact that they were forming alongside a clinker, slag or ash particle, which would confirm the formation of a C-(A)-S-H/C-A-S-H-like mix of gels. Another finding

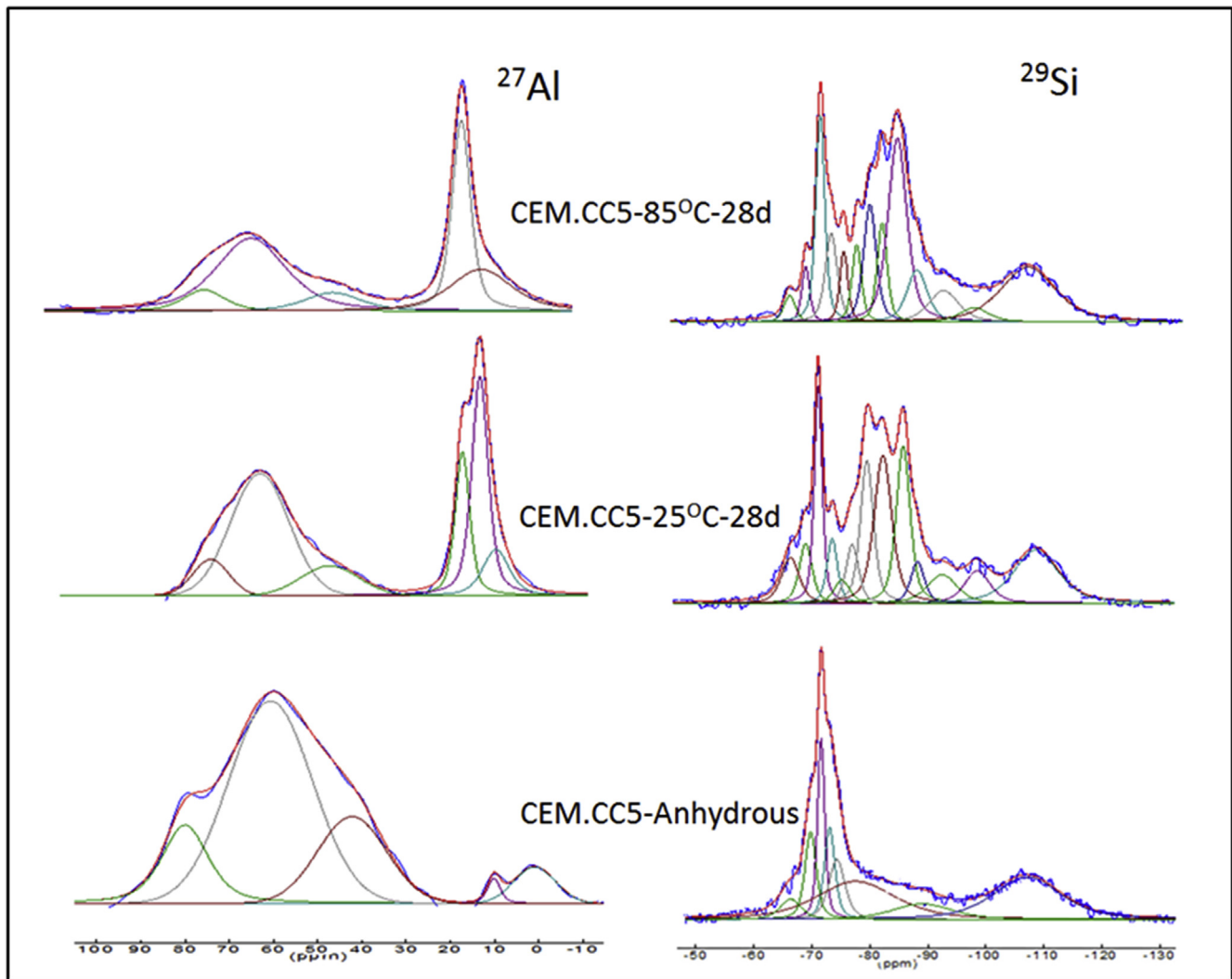


Fig. 8. Deconvolution of (a)  $^{27}\text{Al}$  MAS-NMR and (b)  $^{29}\text{Si}$  MAS-NMR spectra for the anhydrous hybrid cement and its 28-day pastes.

**Table 4**  
Deconvolution of  $^{29}\text{Si}$  MAS-NMR spectra, showing signal position and area.

Sample		Slag		Clinker		Q <sup>1</sup>	Q <sup>2</sup> (1Al)	Q <sup>2</sup>	Q <sup>3</sup> (2Al)	Q <sup>3</sup> (1Al)	Q <sup>3</sup>	FA		
		Q <sup>0</sup>	Q <sup>0</sup>	Q <sup>0</sup>	Q <sup>0</sup>								Q <sup>1</sup>	Q <sup>4</sup>
Anhyd.	Pos.(ppm)	-66.3	-69.8	-71.6	-73.0	-74.3	-77.6		-89.0 <sup>a</sup>			-107.1		
	Integration(%)	3.72	8.67	11.34	8.45	8.5	26.16		8.03			25.11		
25 °C	Pos.(ppm)	-67	-69.5	-71.6	-73.9	-75.5	-77.2	-79.6	-82.3	-85.6	-87.9	-92.2	-97.8	107.4
	Integration(%)	5.01	4.68	10.59	4.13	2.2	4.52	11.36	15.97	13.29	3.47	5.2	5.04	14.54
85 °C	Pos.(ppm)	-66.3	-69.1	-71.5	-73.4	-75.5	-77.7	-79.9	-82	-84.6	-87.9	-92.4	-97.6	106.7
	Integration(%)	1.91	2.70	10.41	6.67	3.57	4.47	9.17	6.07	21.44	6.56	5.85	2.58	18.61

<sup>a</sup> Signal for a phase in fly ash, possibly mullite.

worthy of note was the presence of a small amount of Na (see microanalysis), sourced from the alkaline activator (CC5) used to manufacture the cement. The sodium was fixed in the cementitious gel to balance the charge deficit generated when a silicon tetrahedron was replaced by an aluminium tetrahedron.

As far as the effect of temperature is concerned, the XRD analyses detected no ettringite at any age (3, 28 or 90 days) in the pastes pre-cured at 85 °C for 20 h. Nonetheless, SEM revealed the presence of sulfates throughout the matrix, in all likelihood the result of the adsorption of the sulfates present in the aqueous phase

onto the gel surface (see points 3 and 4). Many of the references in the literature to the uptake of sulfate ions on/into the C-S-H gel surface/structure [32,33] report that this development is favoured by the presence of alkalis and high curing temperatures. Nonetheless, the impact of the sulfate ions absorbed onto the gel structure has yet to be determined. In contrast, the risk posed by the release of those ions at mature cement ages and concomitant delayed ettringite formation (DEF) is better understood [34,35].

The calorimetric and XRD findings indicated that raising the curing temperature from 25 to 85 °C in the first 20 h of the reaction

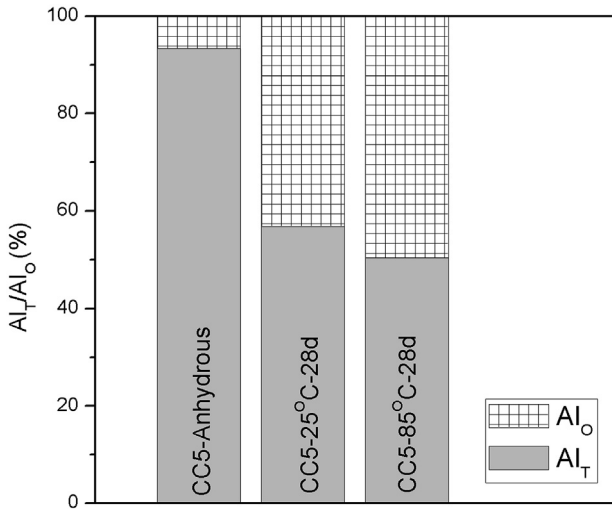


Fig. 9. Sums of Al<sub>T</sub> and Al<sub>O</sub> signals (in per cent).

expedites initial hydration in hybrid cement. That would explain the high 3-day mechanical strength values ( $\approx 30$  MPa). At longer reaction times, however, the beneficial effect of a higher pre-curing temperature was attenuated, whereas in the mortars pre-cured at ambient temperature mechanical strength continued to rise, with 28- and 90-day values of 35 and 40 MPa, respectively. That may be because the reaction products that formed rapidly in the cements pre-cured at 85 °C built a barrier around the unreacted particles, delaying their hydration [24,36].

The variations revealed by NMR and SEM in the composition and structure of the gels also merit comment. When initial curing took place at 85 °C, more C-A-S-H than C-(A)-S-H gel formed. High curing temperature and the presence of alkalis are known to hasten calcium silicate hydration in clinker and C-S-H gel nucleation, although these two parameters also lower calcium hydroxide solubility [32,33] and consequently the amount of this compound available for ettringite formation. At the same time, higher temperature and alkalis raise the solubility of the Si and Al in SCMs [24] (ash and slag in this case). Therefore, with the rise in pre-curing temperature, the aqueous phase would be expected to contain larger amounts of Si and Al ions and smaller amounts of Ca ions. That would favour the speedier precipitation of C-A-S-H than C-(A)-S-H gels. C-A-S-H gel formation around unreacted particles early into the reaction would explain the high 3-day strength observed in the cement pre-cured at 85 °C. This possibly less permeable gel would hamper the diffusion and subsequent hydration of anhydrous particles, however, explaining the lesser rise in mechanical strength observed.

4. Conclusions

This report on a pre-industrial hybrid cement with a low clinker content manufactured with an alkaline activator shows that the production of cement with a very low clinker factor and high mechanical strength is feasible. The material in question set and hardened at ambient temperature, giving rise to a binder with higher mechanical strength than required for general purpose cement (UG) under Colombian standard NTC 121, and for class 32.5 cement defined in European standard EN 196-1.

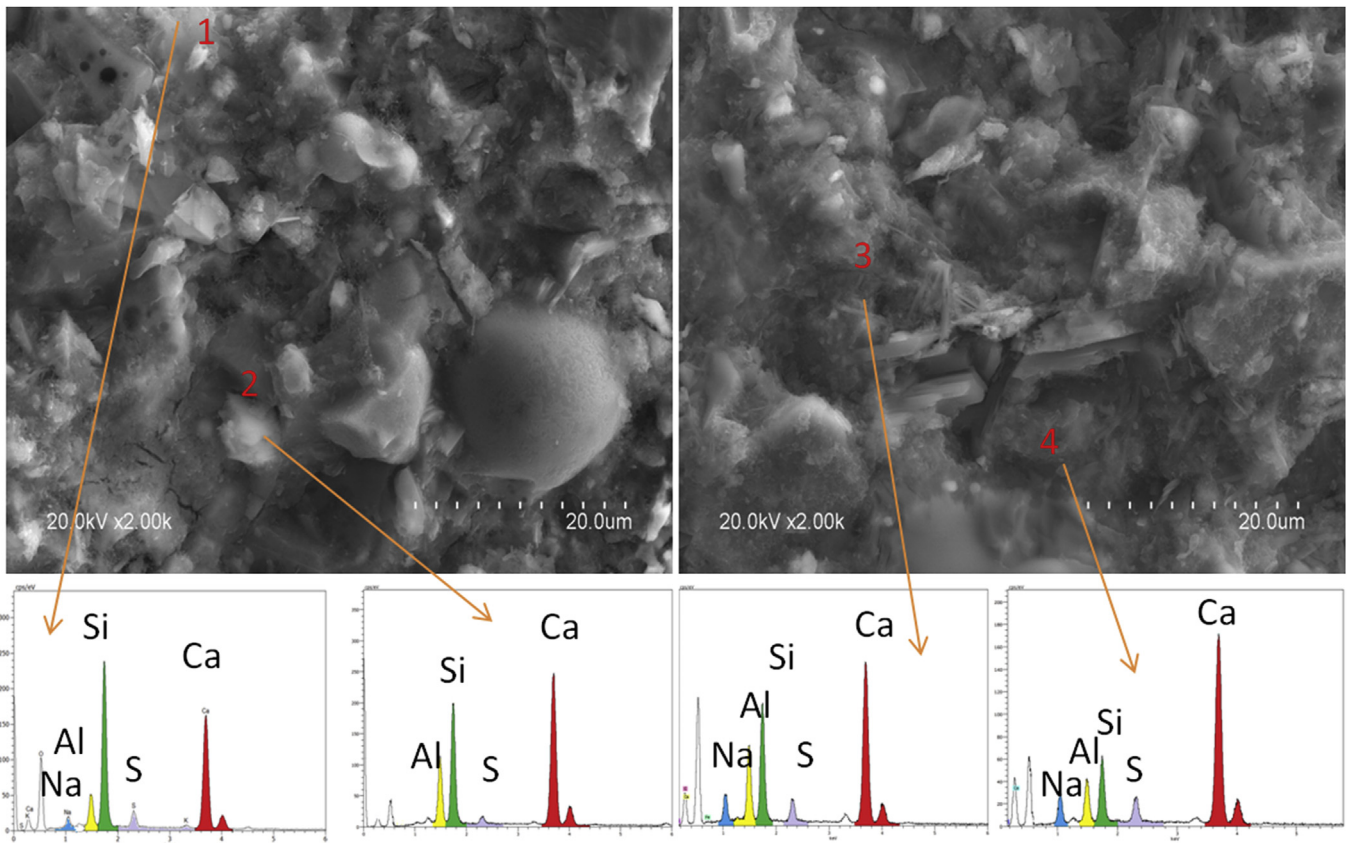


Fig. 10. SEM micrographs and EDX analysis of 28-day CEM CC5 pre-cured at: (a) 25 °C; (b) 85 °C.

Hybrid cement owes its good mechanical strength to the main hydration product, a mix of cementitious gels C-(A)-S-H + C-A-S-H. These gels take up a larger percentage of aluminium and are more intensely polymerised than traditional C-S-H gel.

In hybrid cement a high pre-curing temperature expedites hydration reactions in much the same way as in OPC and alkaline cements. Raising the temperature from 25 to 85 °C accelerated the initial reaction in the cement studied, which exhibited 3-day compressive strength values of up to 30 MPa. Nonetheless, the subsequent development of mechanical strength was slower than when the cement was pre-cured at ambient temperature. Initial curing at 85 °C for 20 h induced the formation of more polymerised gels (lower ratio) and inhibited ettringite formation (or favoured its swift decomposition), at least during the first 90 days, the maximum age of the materials analysed here. The possibility of delayed ettringite formation (DEF) at later ages in these thermally pre-cured hybrid cements cannot therefore be ruled out.

### Acknowledgements

Funding for this research was provided by the Spanish Ministry of the Economy and Competitiveness under projects BIA2013-43293-R, RTC-2014-2351-5 and MAT2012-38541-C02-02), Comunidad de Madrid (S2013/MIT-2862-MULTIMAT CHALLENGE). Author QuBo, a PhD. student, worked under a China Scholarship Council grant.

### References

- [1] M. Schneider, M. Romer, M. Tschudin, H. Bolio, Sustainable cement production—present and future, *Cem. Concr. Res.* 41 (2011) 642–650.
- [2] H.F.W. Taylor, *Cement Chemistry*, Thomas Telford, London, 1997.
- [3] <https://www.oficemen.com>, in.
- [4] C. Shi, A.F. Jiménez, A. Palomo, New cements for the 21st century: the pursuit of an alternative to Portland cement, *Cem. Concr. Res.* 41 (2011) 750–763.
- [5] A. Palomo, P. Krivenko, I. Garcia-Lodeiro, E. Kavalerova, O. Maltseva, A. Fernández-Jiménez, A Review on Alkaline Activation: New Analytical Perspectives, 2014.
- [6] C. Shi, P.V. Kriveoko, D. Roy, *Alkali-activated Cements and Concretes*, first ed., Taylor & Francis, Abingdon, UK, 2006.
- [7] F. Pacheco-Torgal, J.A. Labrincha, C. Leonelli, A. Palomo, P. Chindapasirt (Eds.), *Handbook of Alkali-activated Cements, Mortars and Concretes*, Woodhead Publishing, Oxford, 2015, pp. i–iii.
- [8] B. Lothenbach, K. Scrivener, R.D. Hooton, Supplementary cementitious materials, *Cem. Concr. Res.* 41 (2011) 1244–1256.
- [9] A. Schöler, B. Lothenbach, F. Winnefeld, M. Zajac, Hydration of quaternary Portland cement blends containing blast-furnace slag, siliceous fly ash and limestone powder, *Cem. Concr. Compos.* 55 (2015) 374–382.
- [10] O. Kayali, M. Sharfuddin Ahmed, Assessment of high volume replacement fly ash concrete- Concept of performance index, *Constr. Build. Mater.* 39 (2013) 71–76.
- [11] A. Durán-Herrera, C.A. Juárez, P. Valdez, D.P. Bentz, Evaluation of sustainable high-volume fly ash concretes, *Cem. Concr. Compos.* 33 (2011) 39–45.
- [12] I. García-Lodeiro, A. Fernández-Jiménez, A. Palomo, Variation in hybrid cements over time. Alkaline activation of fly ash—portland cement blends, *Cem. Concr. Res.* 52 (2013) 112–122.
- [13] S. Alarache, F. Winnefeld, J.B. Champenois, F. Hesselbarth, B. Lothenbach, Chemical activation of hybrid binders based on siliceous fly ash and Portland cement, *Cem. Concr. Compos.* 66 (2016), 10e23.
- [14] S. Donatello, O. Maltseva, A. Fernandez-Jimenez, A. Palomo, The early age hydration reactions of a hybrid cement containing a very high content of coal bottom ash, *J. Am. Ceram. Soc.* 97 (3) (2014) 929–937.
- [15] S.-D. Wang, K.L. Scrivener, P.L. Pratt, Factors affecting the strength of alkali-activated slag, *Cem. Concr. Res.* 24 (1994) 1033–1043.
- [16] A. Fernández-Jiménez, J.G. Palomo, F. Puertas, Alkali-activated slag mortars: mechanical strength behaviour, *Cem. Concr. Res.* 29 (1999) 1313–1321.
- [17] S.A. Bernal, R. Mejía de Gutiérrez, J.L. Provis, Engineering and durability properties of concretes based on alkali-activated granulated blast furnace slag/metakaolin blends, *Constr. Build. Mater.* 33 (2012) 99–108.
- [18] Á. Palomo, S. Alonso, A. Fernandez-Jiménez, I. Sobrados, J. Sanz, Alkaline activation of Fly Ashes: NMR study of the reaction products, *J. Am. Ceram. Soc.* 87 (2004) 1141–1145.
- [19] M. Criado, A. Fernández-Jiménez, A. Palomo, Alkali activation of fly ash. Part III: effect of curing conditions on reaction and its graphical description, *Fuel* 89 (2010) 3185–3192.
- [20] J. Hirrljac, Z.Q. Wu, J.F. Young, Silicate polymerization during the hydration of alite, *Cem. Concr. Res.* 13 (1983) 877–886.
- [21] J.I. Escalante-García, J.H. Sharp, Variation in the composition of C-S-H gel in Portland cement pastes cured at various temperatures, *J. Am. Ceram. Soc.* 82 (1999) 3237–3241.
- [22] I.F. Sáez del Bosque, S. Martínez-Ramírez, M.T. Blanco-Varela, FTIR study of the effect of temperature and nanosilica on the nano structure of C-S-H gel formed by hydrating tricalcium silicate, *Constr. Build. Mater.* 52 (2014) 314–323.
- [23] M.A.G. Aranda, Á.G. De la Torre, L. León-Reina, Rietveld quantitative phase analysis of OPC clinkers, cements and hydration products, *Rev. Mineral. Geochem.* 74 (2012) 169–209.
- [24] J.I. Escalante-García, J.H. Sharp, The effect of temperature on the early hydration of Portland cement and blended cements, in: *Advances in Cement Research*, 2000, pp. 121–130.
- [25] C. Shi, R.L. Day, A calorimetric study of early hydration of alkali-slag cements, *Cem. Concr. Res.* 25 (1995) 1333–1346.
- [26] I. Garcia-Lodeiro, A. Fernandez-Jimenez, A. Palomo, Hydration kinetics in hybrid binders: early reaction stages, *Cem. Concr. Compos.* 39 (2013) 82–92.
- [27] I. Garcia-Lodeiro, A. Palomo, A. Fernández-Jiménez, D.E. Macphee, Compatibility studies between N-A-S-H and C-A-S-H gels. Study in the ternary diagram Na<sub>2</sub>O–CaO–Al<sub>2</sub>O<sub>3</sub>–SiO<sub>2</sub>–H<sub>2</sub>O, *Cem. Concr. Res.* 41 (2011) 923–931.
- [28] A. Fernández-Jiménez, F. Puertas, I. Sobrados, J. Sanz, Structure of calcium silicate hydrates formed in alkaline-activated slag: influence of the type of alkaline activator, *J. Am. Ceram. Soc.* 86 (2003) 1389–1394.
- [29] M.D. Andersen, H.J. Jakobsen, J. Skibsted, Incorporation of aluminum in the calcium silicate hydrate (C–S–H) of hydrated portland cements: a high-field 27Al and 29Si MAS NMR investigation, *Inorg. Chem.* 42 (2003) 2280–2287.
- [30] I.G. Richardson, G.W. Groves, The structure of the calcium silicate hydrate phases present in hardened pastes of white Portland cement/blast-furnace slag blends, *J. Mater. Sci.* 32 (1997) 4793–4802.
- [31] J. Schneider, M.A. Cincotto, H. Panepucci, 29Si and 27Al high-resolution NMR characterization of calcium silicate hydrate phases in activated blast-furnace slag pastes, *Cem. Concr. Res.* 31 (2001) 993–1001.
- [32] Y. Fu, P. Xie, P. Gu, J.J. Beaudoin, Effect of temperature on sulphate adsorption/desorption by tricalcium silicate hydrates, *Cem. Concr. Res.* 24 (1994) 1428–1432.
- [33] J.J. Thomas, D. Rothstein, H.M. Jennings, B.J. Christensen, Effect of hydration temperature on the solubility behavior of Ca-, S-, Al-, and Si-bearing solid phases in Portland cement pastes, *Cem. Concr. Res.* 33 (2003) 2037–2047.
- [34] H.F.W. Taylor, C. Famy, K.L. Scrivener, Delayed ettringite formation, *Cem. Concr. Res.* 31 (2001) 683–693.
- [35] M. Collepardi, A state-of-the-art review on delayed ettringite attack on concrete, *Cem. Concr. Compos.* 25 (2003) 401–407.
- [36] J.I. Escalante-García, J.H. Sharp, The microstructure and mechanical properties of blended cements hydrated at various temperatures, *Cem. Concr. Res.* 31 (2001) 695–702.